# Supporting Information

Shroff et al. 10.1073/pnas.0900914106

## SI Text

**Details of Mass Spectrometry Measurements.** *Identification of ions.* The identities of ions were confirmed by accurate mass measurements, isotope distribution analysis, and, wherever possible, with collision-induced-dissociation (CID) studies. Accurate mass measurements were made by using external as well as internal calibration and further on lock-mass correction of the spectra based on the *m*/*z* values of the internal calibrants. The above mentioned criteria provided a mass accuracy of 0.02 Da in all cases. Further, for identification of metabolites from *Arabidopsis thaliana* leaf, each peak was queried against the KNApsAcK *A. thaliana* metabolomic database (http://prime.psc.riken.jp/?action=metabolites_index) accessible via TAIR—The *Arabidopsis* information resource: www.arabidopsis.org/.

**Details of Density Functional Theory Calculations.** *Computational details.* All quantum chemical calculations were performed at the density functional theory (DFT) level. Geometry optimizations were carried out at the Perdew–Burke–Ernzerhof (PBE) level (1). The DFT/PBE calculations were expedited by expanding the Coulomb integrals in an auxiliary basis set, the resolution-of-identity (RI-J) approximation (2, 3). The def2-SVP basis set was used on all atoms (4, 5). Accurate single-point energies were then calculated by using the B3LYP method (6–8) as implemented in Turbomole 5.8 (9). For these calculations, the def2-TZVP basis set was used on all atoms (4). For the reference reactions in solvent, the coupled cluster (CC2) method was used using aug-cc-pVDZ (10) and aug-cc-VTZ (11) basis sets. To allow for solvation effects, the conductor-like screening model (COSMO) method (12, 13), was used with the dielectric constant corresponding to ethanol ($\varepsilon_r = 24.55$). The Gibbs free energy was then calculated as the sum of the following contributions:

$$G = E_{el} + G_{\text{solv}} + E_{\text{ZPE}} - RT\,\ln(q_{\text{trans}}\,q_{\text{rot}}\,q_{\text{vib}}), \qquad \textbf{[s1]}$$

where $E_{el}$ is the in vacuo energy of the system, $G_{\text{solv}}$ is the solvation free energy, $E_{\text{ZPE}}$ is the zero-point energy, and $-RT\,\ln(q_{\text{trans}}\,q_{\text{rot}}\,q_{\text{vib}})$ accounts for the entropic terms and the thermal correction to the enthalpy obtained from a frequency calculation at 298 K and 1 atm using the ideal-gas approximation (14).

1. Perdew JP, Burke K, Ernzerhof M (1996) Generalized gradient approximation for the exchange-correlation hole of a many-electron system. *Phys Rev Lett* 77:3865–3868.
2. Eichkorn K, Treutler O, Öhm H, Häser M, Ahlrichs R (1995) Auxiliary basis-sets to approximate Coulomb potentials. *Chem Phys Lett* 240:283–290.
3. Eichkorn K, Weigen F, Treutler O, Ahlrichs R (1997) Auxiliary basis sets for main row atoms and transition metals and their use to approximate Coulomb potentials. *Theor Chim Acta* 97:119–124.
4. Weigend F, Ahlrichs R (2005) Balanced basis sets of split valence, triple zeta valence and quadruple zeta valence quality for H to Rn: Design and assessment of accuracy. *Phys Chem Chem Phys* 7:3297–3305.
5. Schäfer A, Huber C, Ahlrichs R (1994) Fully optimized contracted Gaussian-basis sets of triple zeta valence quality for atoms Li to Kr. *J Chem Phys* 100:5829–5835.
6. Becke AD (1988) Density-functional exchange-energy approximation with correct asymptotic-behavior. *Phys Rev A* 38:3098–3100.
7. Becke AD (1993) Density-functional thermochemistry: 3. The role of exact exchange. *J Chem Phys* 98:5648–5652.
8. Stephens PJ, Devlin FJ, Frisch MJ, Chabalowski CF (1994) Ab-initio calculations of vibrational absorbtion and circular-dichroism spectra using density-functional force-fields. *J Phys Chem* 98:11623–11627.
9. Hertwig RH, Koch W (1997) On the parameterization of the local correlation functional. What is Becke-3-LYP? *Chem Phys Lett* 268:345–351.
10. Woon DE, Dunning TH (1993) Gaussian-basis sets for use in correlated molecular calculations. 3. The atoms aluminium thorough argon. *J Chem Phys* 98:1358–1371.
11. Kendall RA, Dunning TH, Harrison RJ (1992) Electron-affinities of the 1st-row atoms revisited—Systematic basis-sets and wave-functions. *J Chem Phys* 96:6796–6806.
12. Klamt A, Schuurmann G (1993) COSMO—A new approach to dielectric screening in solvents with explicit expressions for the screening energy and its gradient. *J Chem Soc Perkin Trans* 2:799–805.
13. Schäfer A, Klamt A, Sattel D, Lohrenz JCW, Eckert F (2000) COSMO Implementation in TURBOMOLE: Extension of an efficient quantum chemical code towards liquid systems. *Phys Chem Chem Phys* 2:2187–2193.
14. Jensen F (1999) *Introduction to Computational Chemistry* (Wiley, New York).

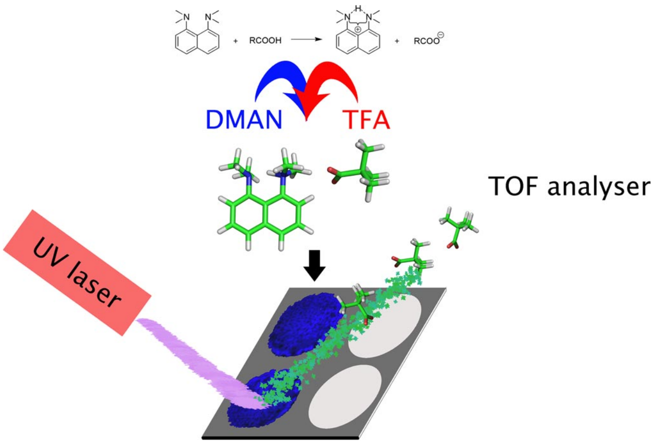

**Fig. S1.** Schematic illustration of the principle of matrix-assisted ionization/laser desorption (MAILD) mass spectrometry; interaction between DMAN and the acidic analytes, e.g., DMAN$+$H$^+$CF$_3$COO$^-$ salt; its minimum energy structure calculated by DFT, corresponding to the X-ray determined structure, is shown.

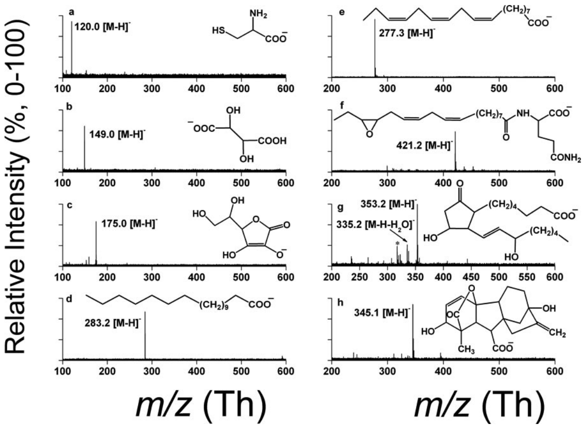

**Fig. S2.** MAILD TOF/MS negative-ion spectra of 100 pmol of a) cysteine (*A*), tartaric acid (*B*), ascorbic acid (*C*), stearic acid (*D*), linolenic acid (*E*), N-(15,16-epoxylinolenoyl)glutamic acid (*F*), alprostadil (*G*), and gibberellic acid (*H*) (100 pmol each). The asterisk denotes the peak at *m/z* 335.2 corresponding to loss of 1 water molecule from the deprotonated alprostadil $[M\text{-}H\text{-}H_2O]^-$. The plus mark denotes the peak corresponding to *m/z* 317.2 $[M\text{-}H\text{-}2H_2O]^-$.

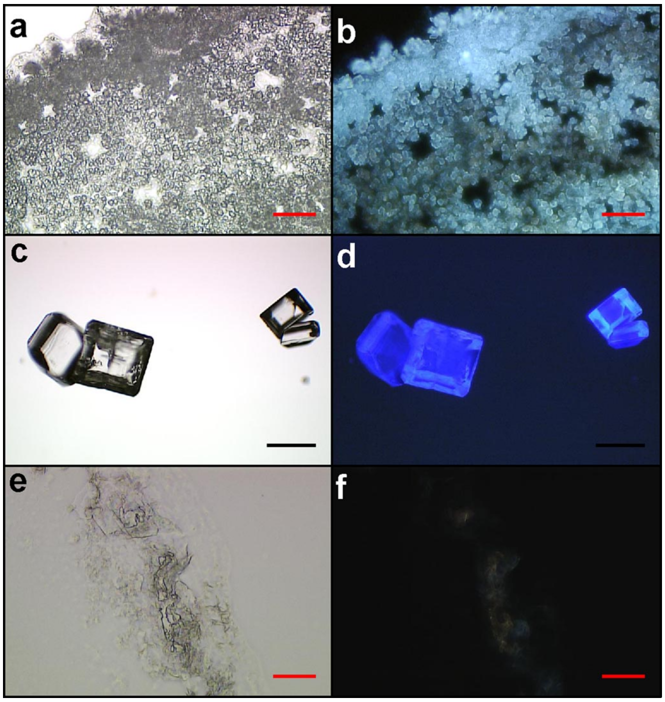

**Fig. S3.** (*a*, *c*, and *e*) Optical images for DMAN crystals (*a*), crystals obtained after mixing DMAN and TFA (*c*), and crystals obtained after mixing DMAN and SA (*e*). (*b*, *d*, and *f*) Fluorescence images for DMAN crystals (*b*), crystals obtained after mixing DMAN and TFA (*d*), and crystals obtained after mixing DMAN and SA (*f*). (Red scale bar, 25 $\mu$m; black scale bar, 310 $\mu$m.)

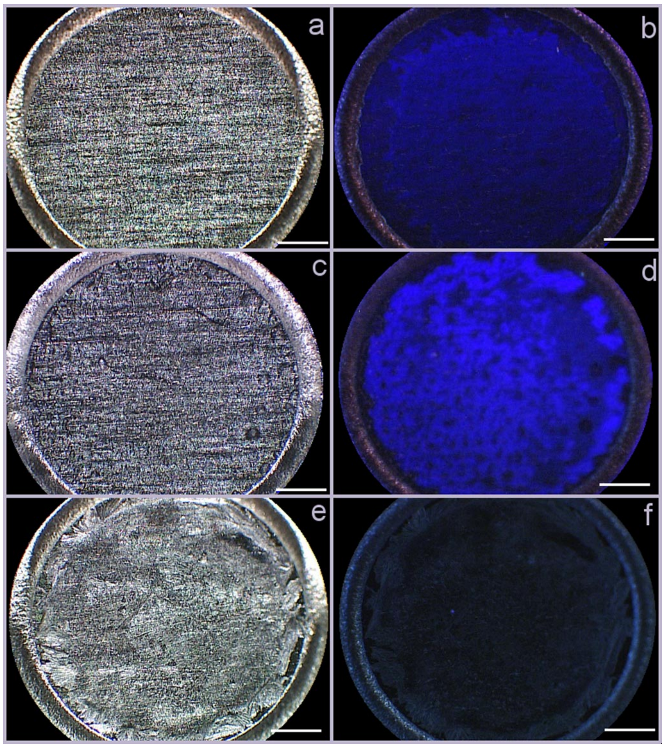

**Fig. S4.** Images showing the surface coverage of DMAN and DMAN with analytes on a MALDI metallic plate. (*a*, *c*, and *e*) The optical images of DMAN (*a*), DMAN + TFA (*c*), and DMAN + SA (*e*). (*b*, *d*, and *f*) The fluorescent images of DMAN (*b*), DMAN + TFA (*d*), and DMAN + SA (*f*).

**Table S1. Comparison of the list of metabolites (fatty acids, FA) identified from 2:1 $CHCl_3$:$CH_3OH$ extracts of 7 *Drosophila melanogaster* males through MAILD-TOF/MS (untreated as FA) and GC-MS as FA methyl esters (FAME) prepared by diazomethane treatment**

| FA* identified through MALDI-MS | Analytes identified through GC-MS |
|---|---|
| 12:0, 14:0, 14:1, 16:0, 16:1, 17:2, 18:0, 18:1, 18:2, 18:3, 19:0, 19:2, 19:3, 20:1, 20:2, 20:3, 21:0, 21:1, 21:2, 22:3, 22:0, 22:1, 23:0, 23:2, 24:0, 25:0, 29:6, 30:5, 33:2, 33:4, 39:4 | 12:0, 14:0, 14:1, 15:0, 15:1, 16:0, 16:1, 18:0, 18:1 |

The same number of metabolites could be identified by using MAILD-TOF/MS even from a single fly; however, in the case of a single fly extract, GC-MS sensitivity was insufficient to allow for the observation of any metabolites.

*The numbers before colons refer to the number of carbons and those after the colons refer to the number of double bonds; 18:1 is oleic acid.

**Table S2. The calculated proton affinities ($\Delta G_{pa}$) and Gibbs energies of deprotonation ($\Delta G_{deprot}$) of neutral species in gas phase and in solvent (ethanol)**

| | Gas phase | | | Solvent (ethanol) | | |
|---|---|---|---|---|---|---|
| | $\Delta G_{pa}$ | $\Delta G_{deprot}$ | $\Delta G_{pa}$ | p$K_a$ | $\Delta G_{deprot}$ | p$K_a$ |
| Aniline | 210.0 | 368.3 | 267.8 | 3.3 | 318.5 | 40.4 |
| DAN | 224.9 | 352.8 | 269.7 | 4.6 | 310.3 | 34.3 |
| DMA | 222.2 | 398.5 | 270.1 | 4.9 | 347.4 | 61.5 |
| DMAN | 245.3 | 393.0 | 282.5 | 13.6 | 351.5 | 64.6 |
| DMAN-Ac | n/a | 353.1 | n/a | n/a | 311.4 | 35.2 |
| Naptho-$SO_3H$ | 194.5 | 313.9 | 236.0 | −20.5 | 266.5 | 2.3 |

The values are in kcal.mol$^{-1}$ or in dimensionless p$K_a$ scale (p$K_a$). The free energy of proton solvation in methanol was used ($\Delta G_{solv}(H^+) = 263.4$ kcal.mol$^{-1}$) for the p$K_a$ scale[24]. DAN represents 1,8-diaminonaphthalene, DMA *N*,*N*-dimethylaniline, DMAN 1,8-bis(dimethylamino)naphthalene, and DMAN-Ac corresponds to the salt of DMAN with acetic acid used as a simple model for preliminary calculations. n/a, not applicable.

**Table S3. The calculated Gibbs free energies of salt formation in ethanol (AH…B → $A^-$…$BH^+$ reaction), $\Delta G_{\text{salt-form}}$, and the total Gibbs free energy of ionization, $\Delta G_{\text{ion}}$**

| Complex with<br>DMAN | $\Delta G_{\text{salt-form}}$ (ethanol)<br>[$\text{kcal·mol}^{-1}$] | $\Delta G_{\text{ion}}$<br>[$\text{kcal·mol}^{-1}$] |
|---|---|---|
| $CF_3COOH$ | −3.7 | −86.8 |
| $CCl_3COOH$ | −2.8 | −84.7 |
| $C(CH_3)_3COOH$ | 1.9 | −94.9 |
| $CH_3COOH$ | 2.2 | −98.3 |

The $\Delta G_{\text{ion}}$ corresponds to the overall process of ionization, i.e., AH…B(*aq*) → $A^-$(*g*) + $BH^+$ (*g*) or $A^-$…$BH^+$(*aq*) → $A^-$(*g*) + $BH^+$ (*g*) (when the zwitterionic form is more stable in solution) processes. DMAN represents 1,8-bis(dimethylamino)naphthalene.

**Table S4. Crystal data and structure refinement for 1,8-bis(dimethylamino)naphthalene trifluoroacetate (fo3376)**

| | | |
|---|---|---|
| Identification code | FO3376 | |
| Empirical formula | $C_{16}H_{19}F_3N_2O_2$ | |
| Formula weight | 328.33 | |
| Temperature | 183(2) K | |
| Wavelength | 0.71073 Å | |
| Crystal system | Orthorhombic | |
| Space group | Pnma | |
| Unit cell dimensions | $a$ = 6.9877(4) Å | $a$ = 90°. |
| | $b$ = 12.4040(7) Å | $b$ = 90°. |
| | $c$ = 19.1110(7) Å | $g$ = 90°. |
| Volume | 1656.45(15) $Å^3$ | |
| $Z$ | 4 | |
| Density (calculated) | 1.317 $Mg/m^3$ | |
| Absorption coefficient | 0.110 $mm^{-1}$ | |
| F(000) | 688 | |
| Crystal size | 0.05 × 0.05 × 0.04 $mm^3$ | |
| $\theta$ -range for data collection | 3.10 to 27.49°. | |
| Index ranges | $-8 \leq h \leq 9$, $-13 \leq k \leq 16$, $-23 \leq l \leq 24$ | |
| Reflections collected | 10,666 | |
| Independent reflections | 1,974 [$R$(int) = 0.0665] | |
| Completeness to $\theta$ = 27.49° | 99.5% | |
| Absorption correction | None | |
| Refinement method | Full-matrix least-squares on $F^2$ | |
| Data/restraint /parameters | 1,974/0/115 | |
| Goodness-of-fit on $F^2$ | 1.063 | |
| Final $R$ indices [$I > 2\sigma(I)$] | $R1$ = 0.1081, $wR2$ = 0.3082 | |
| $R$ indices (all data) | $R1$ = 0.1504, $wR2$ = 0.3503 | |
| Extinction coefficient | 0.019(8) | |
| Largest diff. peak and hole | 1.135 and −0.915 $e·Å^{-3}$ | |

**Table S5. Atomic coordinates (× $10^4$) and equivalent isotropic displacement parameters ($Å^2 \times 10^3$) for fo3376**

| Atom(No) | *x* | *y* | *z* | *U*(eq) |
|---|---|---|---|---|
| N(1) | 7311(4) | 6468(2) | 575(2) | 26(1) |
| C(1) | 8850(5) | 6474(3) | 1089(2) | 24(1) |
| C(2) | 9552(7) | 7500 | 1321(2) | 22(1) |
| C(3) | 11050(7) | 7500 | 1833(2) | 26(1) |
| C(4) | 11745(5) | 6503(3) | 2081(2) | 32(1) |
| C(5) | 11041(6) | 5547(3) | 1854(2) | 34(1) |
| C(6) | 9560(5) | 5531(3) | 1350(2) | 29(1) |
| C(7) | 5514(6) | 5992(4) | 859(2) | 40(1) |
| C(8) | 7879(6) | 5971(3) | −100(2) | 38(1) |
| O(1) | 7334(6) | 1604(3) | 565(2) | 64(1) |
| C(9) | 7143(9) | 2500 | 823(3) | 38(1) |
| C(10) | 6480(20) | 2500 | 1563(4) | 87(4) |
| F(1) | 6073(15) | 1614(6) | 1870(4) | 84(2) |
| F(2) | 4570(19) | 2022(10) | 1598(6) | 142(4) |
| F(3) | 7264(14) | 1748(7) | 1983(4) | 85(2) |

*U*(eq) is defined as one third of the trace of the orthogonalized $U^{ij}$ *tensor.*